Islamic University Journal of Applied Sciences (IUJAS)
https://journals.iu.edu.sa/jesc

Volume VIII, Issue II, December 2026, Pages 127-148

Explainable Machine Learning Framework for Predicting Bond Strength of FRP Bars Embedded in UHPC

Abdulaziz Alqurashi [1] *

[1.] Department of Civil Engineering, Faculty of Engineering, Islamic University of Madinah, 42351, Madinah, Saudi Arabia, amalqurashi@iu.edu.sa

*Corresponding author: (Abdulaziz Alqurashi), *Email Address*: amalqurashi@iu.edu.sa

Abstract

The interfacial performance of advanced composites bars embedded in Ultra-High Performance Concrete (UHPC) is an important factor that controls load transfer and the performance of structural elements. Predicting bond strength is still difficult because it is affected by several factors, such as rebar type, bar profile, bar diameter, bonded length, cover depth, fiber content, UHPC compressive strength, and FRP tensile strength. Therefore, this study uses machine-learning models to estimate the the bonding capacity of FRP bars placed in UHPC Using a collected experimental database of 183 specimens from previous studies. Four machine-learning models were developed and compared, including Linear Regression, Random Trees, Multi-Layer Perceptron, and Locally Weighted Learning. The MLP model gave the best prediction performance, with a correlation coefficient of 0.9466, MAE of 2.3083 MPa, and RMSE of 3.0631 MPa. SHAP analysis showed that embedment length was the most influential variable, followed by bar surface condition, FRP tensile strength, and concrete cover. This confirms that FRP–UHPC bond behavior is controlled by the interaction between bonded length, surface condition, mechanical interlock, and confinement provided by UHPC. Overall, the developed explainable ML framework provides a useful tool for predicting FRP–UHPC bond strength and supporting future UHPC-specific bond models.

Keywords: Ultra High-Performance Concrete; FRP bars; Pull-out behaviour; Machine Learning; Interfacial Mechanics.

https://doi.org/10.63070/jesc.2026.037
Received 02 May 2026; Revised 21 June 2026; Accepted 24 June 2026; Available online 15 July 2026.
Published by Islamic University of Madinah on behalf of ***Islamic University Journal of Applied Sciences.***
This is an open access article published under the Creative Commons Attribution 4.0 International license (CC BY 4.0):https://creativecommons.org/licenses/by/4.0/

1. Introduction

Ultra-high performance concrete (UHPC) is a high Perfomance building material, developed from the reactive powder concrete concept, characterized by very high strength in compression, dense microstructure, and using the fine constituents and admixtures to enhance durability and mechanical performance [1]. Because UHPC can substantially improve structural capacity and longevity, it is being adopted in bridge decks, prestressed girders, segmental joints and other applications worldwide. Concurrently, nonmetallic reinforcement, such as carbon-, glass-, and basalt-fiber-reinforced polymer bars, referred to as CFRP, GFRP, and BFRP bars, respectively, has attracted attention because of its high tensile capacity and reduced susceptibility to corrosion compared with conventional steel reinforcement. [2-3].

Designing durable and efficient structural elements that combine UHPC with FRP bars requires a reliable understanding of their bonding behaviour within the surrounding UHPC matrix. Bond transfer arises from a combination of mechanical interlock, adhesive interaction, and surface friction. Relative contribution of mechanisms depends on bar material and surface topography, matrix composition (including silica fume and discrete fibers), and geometry (bar diameter, rib geometry, embedment length and concrete cover) [4]. Experimental programs from recent literature (including pushout and pull-out investigations) have documented that steel, GFRP and BFRP bars interact with UHPC through distinct mechanisms: steel typically engages UHPC by rib interlock and may induce local UHPC crushing between ribs. On the other hand, FRP bars often exhibit resin-fiber debonding at the bar interface and direction-dependent (orthotropic) surface responses [5]. Microscopy and surface-texture analyses (e.g., gray-level co-occurrence matrix metrics) further show that interfacial damage and energy dissipation are spatially anisotropic for FRP bars, complicating simple, one-dimensional descriptions of bond behavior [6].

Despite significant experimental efforts, key uncertainties persist. Conflicting trends have been reported for the influence of GFRP bar diameter on bonding behaviour some studies report decreasing bond with increasing diameter, while others observe the opposite and relatively few systematic investigations have mapped how UHPC cover thickness interacts with bar size and embedment depth to control the failure mechanism and the bond stress–slip behaviour [7]. Moreover, predictive formulae derived for steel or FRP in normal or high-strength concrete often fail to reproduce measured bond performance for FRP–UHPC combinations, motivating the development of UHPC-specific empirical relations based on targeted experiments [8]. Because the bonding performance of FRP bars embedded in UHPC is influenced by several variables, the available empirical equations may not always give accurate predictions. These parameters include the matrix composition, embedment length, fiber

content, silica fume content, bar diameter, surface type, and UHPC cover. Therefore, machine learning can be used as a useful tool beside the experimental and analytical work. ML can learn the nonlinear relationship between these parameters and the main outputs, such as interfacial resistance, bond stress–slip behaviour, and the observed failure mechanism, without assuming a fixed equation form from the beginning [9]. Also, explainable ML methods can help show which parameters have the most effect on the bond behaviour and how each parameter increases or decreases the predicted bond capacity. This is important because some existing equations may overestimate or underestimate the bonding capacity for FRP bars embedded in UHPC. Therefore, it can improve the prediction accuracy, support the sensitivity analysis, and help guide future experimental studies, especially in the ranges where the available data are limited [10, 11].

Importance of reinforcement–UHPC interface and motivation for FRP The interfacial behaviour of reinforcement embedded in the UHPC controls the capacity and serviceability of reinforced concrete members because displacement compatibility between the reinforcement and matrix must be achieved through a combination of mechanical interlock, adhesive interaction, and surface friction. Durability concerns (notably corrosion of steel) and service demands have therefore motivated the increased use of non-metallic reinforcement such as GFRP, BFRP, and CFRP bars in aggressive environments and for long-lived infrastructure. Comparative studies of steel, GFRP, BFRP, and CFRP bars combined with UHPC reflect this practical interest.

Distinct bond mechanisms for steel versus FRP in UHPC steel deformed bars and FRP bars develop bond with concrete by different dominant mechanisms. Deformed steel bars commonly rely heavily on the mechanical engagement of the ribs with the UHPC; bond failures with steel in UHPC are frequently associated with shear and compressive crushing of UHPC between steel ribs [12]. In contrast, ribbed FRP bars (including helically ribbed GFRP) tend to fail by debonding at the resin–fiber interface or peeling of resin and fibers from the ribs; microscopy of post-pullout surfaces shows resin/fiber peeling for GFRP, indicating an interfacial failure mode distinct from the UHPC crushing typical of steel bars [13]. Furthermore, FRP bars are orthotropic and more sensitive to lateral compressive stresses, which has implications for specimen design (e.g., use of epoxy-grouted steel tubes to prevent local crushing in tests) and for how cover and confinement affect bond in practice.

Effects of UHPC matrix constituents (fibers, silica fume) and microstructure UHPC differs from normal-strength and ordinary high-strength concretes in compressive strength, microstructure (high fines, silica fume content), and use of discrete steel fibers; these matrix attributes alter the contact conditions at the reinforcement interface [14]. Multiple studies show that adding fibers to the matrix generally improves bond strength and post-peak ductility in concrete systems, and UHPC with steel fibers typically yields greater bond strength than comparable matrices without fibers. Silica-fume

content and the UHPC's high compressive strength influence micro-cracking and local crushing behaviour at ribs, and thus modify whether bond is governed by interlock, adhesion, or crushing phenomena [15, 16]. Because compressive strength of UHPC is much higher than ordinary concrete (OC) and because fibers change tensile and fracture processes, the mechanisms controlling FRP bond in UHPC can differ substantially from those in OC [12, 17].

In addition, a few studies have shown the effects of bar size, embedment length, and cover depth on FRP–UHPC bond behavior are not well documented. Experimentally, several samples have been tested helically ribbed GFRP bars in UHPC and reported two failure patterns, which are direct pull-out and splitting pull-out [18-20]; specimens with larger bar diameters and smaller concrete cover thickness showed a tendency to fail through splitting pull-out. They also reported that increasing cover thickness improved bond strength up to a critical cover of about 3–4 d_b, and that the bond capacity increased as the GFRP bar size increased, owing to the greater rib height [21]. A later study confirmed that no clear agreement had been reached regarding the influence of bar size; their tests with GFRP bar diameters from 8 to 25 mm showed that bond strength increased from 8 to 18 mm but decreased from 18 to 25 mm [7]. In addition, not only increasing UHPC cover depth, and fiber content enhanced the bond capacity, but also, with fiber content increasing from 0–2 % improving the capacity by about 74.81%–92.22%**,** while further increase to 3% had limited additional effect [22]. Comparison UHPC with normal concrete for FRP bond empirical studies generally find that embedding FRP rebars in UHPC improves bond strength compared with normal concrete, but the dominant failure mechanism (resin–fiber debonding for FRP) can persist across matrix types [23]. The markedly higher UHPC strength and presence of fibers influence magnitudes of bond stress and the relative contributions of adhesion, interlock and friction; because of these differences, predictive formulas derived for steel or FRP in conventional concrete often fail to capture GFRP–UHPC behaviour and may require UHPC-specific empirical fitting.

Overall, the literature shows that FRP–UHPC bond behavior is controlled by a nonlinear interaction between the bar surface, rib geometry, embedment length, bar diameter, concrete cover, UHPC fiber content, and the mechanical characteristics of the FRP bar. One of strongest finding across the literature is that surface condition and mechanical interlock are usually more important for FRP bars than concrete compressive strength alone [19]. Smooth FRP bars tend to show weaker and more brittle bond behavior, while helically wound, ribbed, or sand-coated bars can develop higher bond strength through friction and mechanical interlock [24]. However, the influence of embedment length, cover thickness, fiber content, and bar diameter is not always consistent because these parameters interact with each other and with the failure mode [20]. Therefore, conventional empirical equations developed for steel reinforcement or FRP bars in (OC) may not be reliable for FRP bars with UHPC. This gap

supports the use of machine-learning models because ML can identify complex nonlinear interactions among several input variables without assuming a fixed equation form. In this context, explainable ML methods such as SHAP are useful because they do not only improve prediction accuracy, but also help identify which parameters control the predicted bond strength and how these parameters are physically related to adhesion, friction, mechanical interlock, confinement, and stress redistribution.

To address this need, this study uses a collected experimental database from previous studies to develop ML models for estimating the bond capacity of FRP bars in UHPC. Multiple machine-learning algorithms are applied and evaluated according to their prediction accuracy. Explainable ML methods are then used to identify the most important variables and to interpret the contribution of each variable on bond capacity. This approach helps clarify the complex and nonlinear relationships controlling FRP–UHPC bond behavior and provides a useful basis for future design-oriented bond models.

2. Methodology

2.1 Structural method

This study adopts a data-driven methodology to estimate the bond capacity of FRP reinforcing bars embedded in (UHPC). The methodology consists of four main stages: database development, data preprocessing, machine-learning model development, and explain the physical behavior of the FRP–UHPC bond system. First, experimental data were collected from earlier published studies that investigated the bonding performance of FRP bars with UHPC. Then, the collected data were cleaned, standardized, and organized into a structured database. Several ML models were trained and evaluated to estimate the ultimate bond strength (τ_u) in Figure 1.

2.2 Data collection and analysis

A database consisting of 183 experimental specimens was constructed from previous studies that studied the bonding performance of UHPC with FRP reinforcing bars. Dataset are collected from [21, 25-31] are summarized in Table-1. These studies were selected because they reported experimental bond data for FRP bars bonded with UHPC or UHPFRC; also provided the main material and geometric parameters required for model development. The database covered different types of FRP reinforcement, including GFRP, CFRP, and BFRP bars. Most of the collected specimens were related to GFRP bars, while the remaining data included CFRP and BFRP bars. The database also included different experimental methods used to evaluate the bond behavior, such as pull-out, push-in, and beam tests. This variation in bar type and test method helps improve the generality of the ML models.

Because the data were collected from different studies, careful preprocessing was required to reduce inconsistencies between the experimental sources. The collected data were checked for missing values, inconsistent units, duplicated entries, and unclear reported results. The units were standardized, where concrete cover, bar diameter, and bonded length were expressed in (mm), while UHPC compressive strength, FRP tensile strength, and ultimate bond strength were expressed in MPa. Categorical variables, such as bar surface, FRP type, and test procedure, were encoded into numerical values before model development.

The main purpose of the data collection stage was to develop a reliable database that includes the principal variables influencing the bonding performance of FRP bars in UHPC. The data were collected from tables, figures, and reported experimental results in the selected studies. When the ultimate bond strength was reported directly, it was used as provided. However, when only the maximum applied load was available, (τ_u) was calculated using the standard average bond stress equation.

Table-1: summarize the distribution of the collected data and the statistical range of the selected variables.

Inputs	Symbol	Unit	Minimum	Maximum	Average	SD
Bar diameter	d_b	mm	7.5	19.10	12.62	3.81
Concrete cover	c	mm	10	150	73.10	34.17
Embedment length	l_d	mm	10	160	62.81	50.88
Fiber content	ρ_f	%	0	2.5	1.44	1.00
UHPC compressive strength	f'_c	MPa	86	202	155.50	27.89
FRP tensile strength	f_r	MPa	728	2480	1379.67	677.80
Ultimate bond strength	τ_u	MPa	10.20	56.24	25.09	9.52

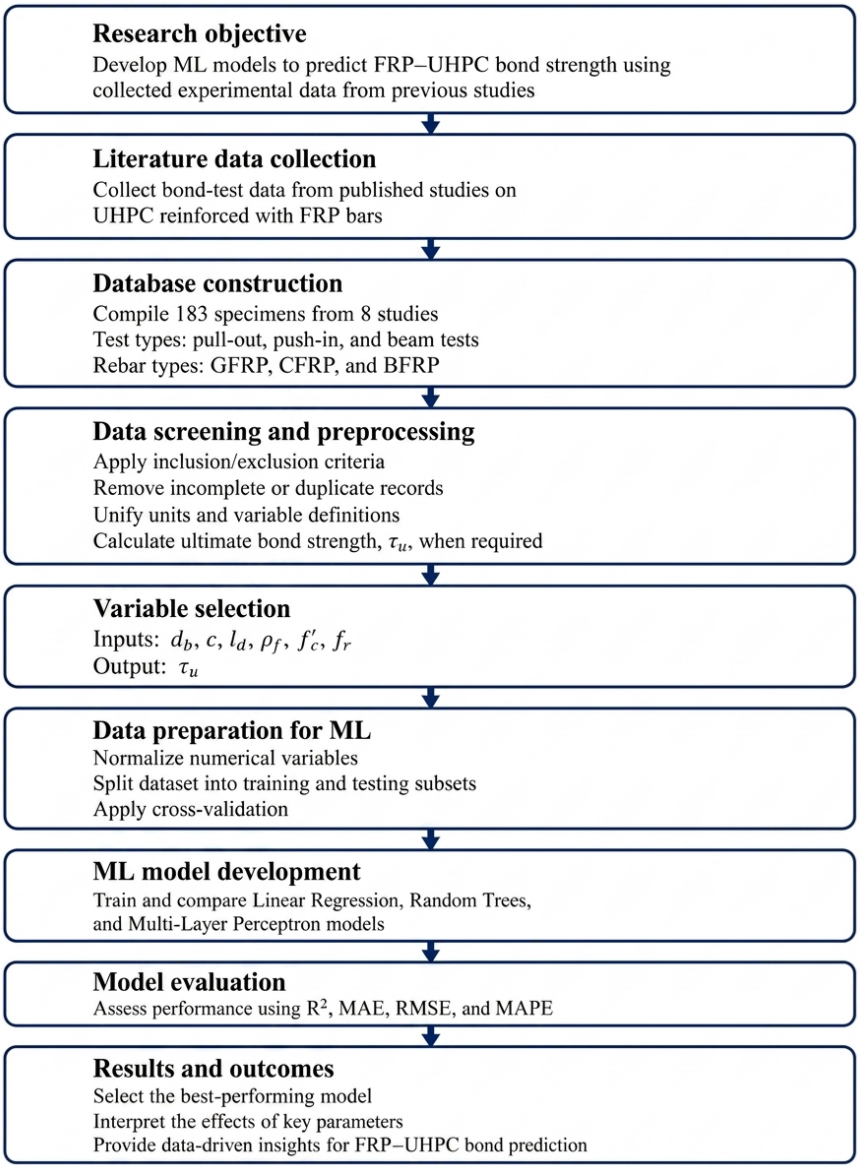


Figure 1. Systematic Workflow for Investigating and Modeling FRP–UHPC Interfacial Bond Performance

2.3 Machine-learning models

Several supervised machine-learning models were developed to predict the ultimate bond strength of FRP bars embedded in UHPC. The selected models included both simple and advanced algorithms to compare their prediction accuracy and ability to capture nonlinear relationships. Four models have been used, which are, Linear Regression (LR), Random Trees (RT), Multi-Layer Perceptron neural network (MLP), and Locally Weighted Learning (LWL). LR was used as a first model because it provides a simple connection the input variables to τ_u. However, τ_u behavior is highly nonlinear because it depends on several interacting parameters, such as concrete strength, fiber content, bar diameter, embedment length, and cover thickness [3, 29, 32, 33]. Therefore, nonlinear ML models were also used. Tree-based models such as Decision Tree, Random Forest, and Gradient Boosting can

capture nonlinear effects and variable interactions. Support Vector Regression can provide good performance for small to medium-size datasets, while the Multi-Layer Perceptron model can learn complex nonlinear relationships through one or more hidden layers coupled with nonlinear activation functions [34]. A correlation matrix was developed to evaluate the linear relationship of the inputs and bond strength. The analysis included bar surface, concrete cover, bar size, bonded length, fiber content, concrete compressive strength, bar tensile strength, and bond strength. Since bar surface is a categorical variable, it was converted into numerical labels before analysis. The heatmap was used to visualize the strength and direction of the correlations. As shown in Figure 2, positive coefficients indicate direct associations, whereas negative coefficients represent inverse associations. Final dataset was separated into training and testing subsets. Training subset was used to develop ML models, whereas testing subset was compared to evaluate the prediction performance. The dataset was split to 80 and 20% for training and testing, respectively. Because the database is relatively limited, cross-validation should also be applied to improve the reliability of the performance evaluation and reduce the effect of random data splitting. For each model, the training process was conducted using the selected input variables and the target bond strength. Hyperparameters were tuned to improve model accuracy and reduce overfitting. The final model parameters were selected based on the performance on the validation or cross-validation results. To ensure a fair comparison, the four models were trained and tested using the same dataset split and the same performance metrics.

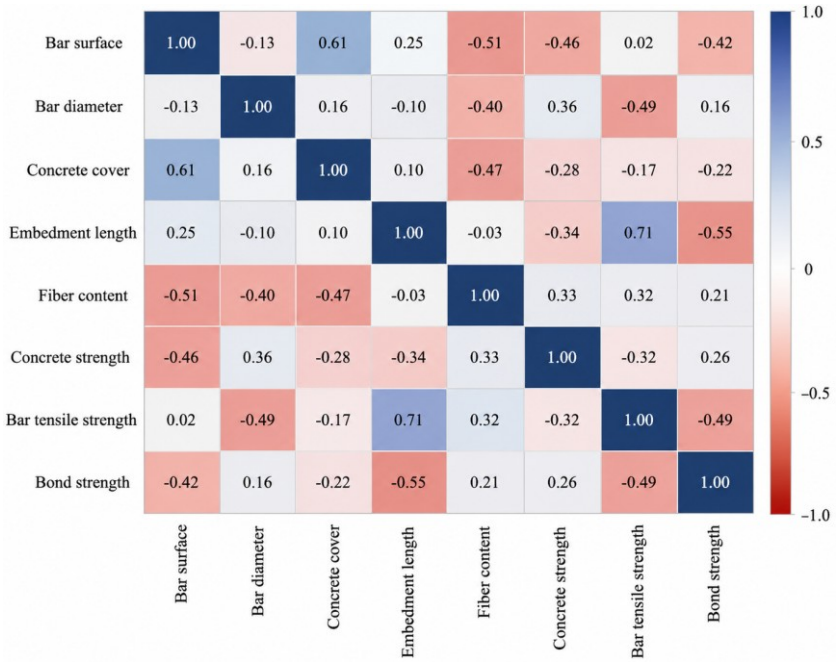


Figure 2. Representing correlation matrix heatmap for collective Dataset.

2.3.1 Random Trees (RT)

Random Trees constitute a powerful supervised machine learning approach that is particularly well suited to capturing nonlinear relationships in engineering datasets. In the context of structural and materials engineering, Random Trees are well suited for predicting performance characteristics where multiple interacting variables influence the response Figure 3. RT algorithm was employed to predict the (τ_u) between FRP and (UHPC), a problem characterized by significant parametric uncertainty and nonlinear interactions among governing variables such as bar size, concrete cover, bonded length, reinforcement type, and surface condition. Random Trees model is an ensemble-based learning technique derived from decision trees algorithms. It constructs multiple decision trees during the training phase using randomly selected subsets of input variables and data samples. Each individual trees generates a prediction, and the last output is obtained by aggregating these estimated values, typically through averaging. This randomness in feature selection and data sampling enhances model robustness and reduces the likelihood of overfitting, a common limitation of single decision trees models. Consequently, Random Trees can capture complex variable interactions and nonlinear dependencies while maintaining strong generalization capability for unseen data.

In the present research, the Random Trees model was trained using experimentally generated bond strength data. the prediction accuracy was evaluated through statistical metrics including the correlation coefficient, mean absolute error, and root mean squared error. The model showed dependable estimation accuracy and offered useful information about the relative contribution of the input variables to bond performance. A key advantage of Random Trees is their inherent can rank input variable importance, thereby assisting in identifying the most influential parameters governing bond strength. This capability supports engineering interpretation and facilitates the development of optimized design strategies. Overall, the Random Trees approach offers a reliable and transparent data-driven approach for estimating interfacial bonding performance in advanced composite–concrete systems.

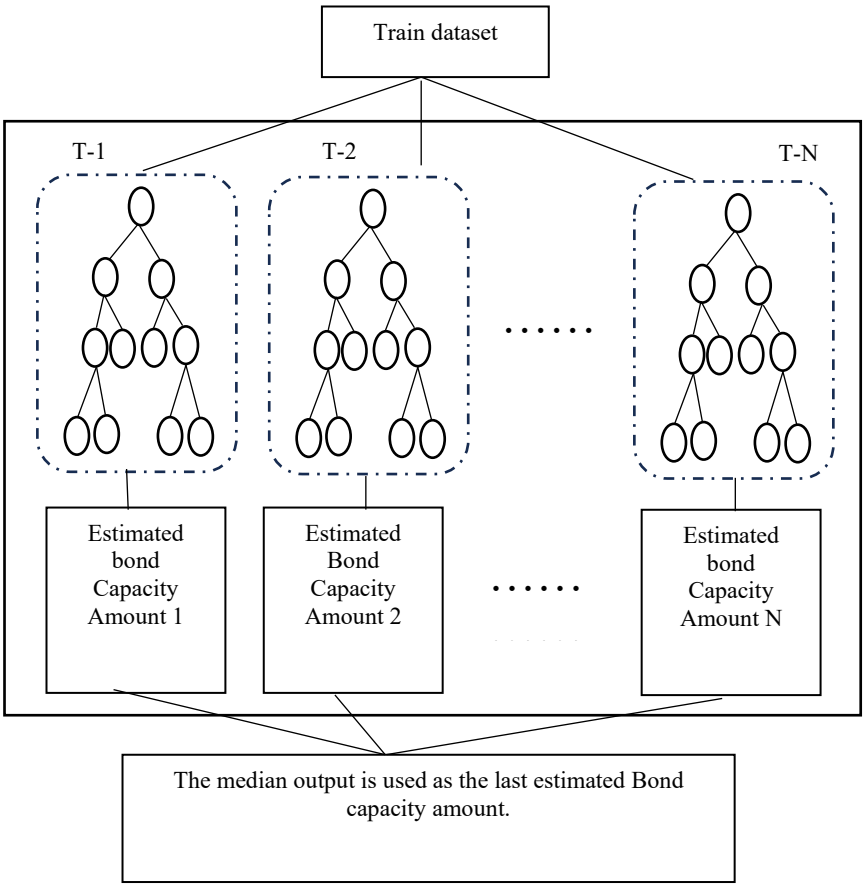


Figure 3. Random Trees diagram

2.3.2 Multi-Layer Perceptron

(MLP) is a feedforward supervised neural network that approximates complex, nonlinear relationships between the input variables and the target outputs by composing multiple layers of linear transforms and elementwise nonlinear activation functions. In the present study, an MLP surrogate was trained to predict bond outcomes (e.g., mean ultimate bond stress or τ_u) from experimental and derived inputs such as reinforcement type and surface, bar diameter, development length, concrete cover, load factor and texture/diagnostic metrics. The MLP's capacity to learn high-order interactions makes it particularly well suited for UHPC-FRP bond problems, where adhesion, friction and mechanical interlock interact nonlinearly and where matrix constituents, bar geometry and surface texture jointly influence failure modes (as discussed in the literature review). In this research, the MLP model was trained using experimentally derived datasets to develop a predictive connections of governing values and ultimate bond strength. The performanceof the model was evaluated using statistical indicators such as correlation coefficient, mean absolute error, and root mean squared error. MLP achieved higher prediction accuracy than conventional linear regression and tree-based models, indicating its strong capability in modeling nonlinear interfacial behavior in composite structural systems. The

implementation of MLP not only enhances prediction reliability but also supports the development of data-driven design tools for UHPC–FRP bonded systems. Consequently, the MLP-based framework provides an efficient and robust approach for understanding and predicting bond behavior, contributing to the advancement of intelligent modeling techniques in modern structural engineering research Figure 4.

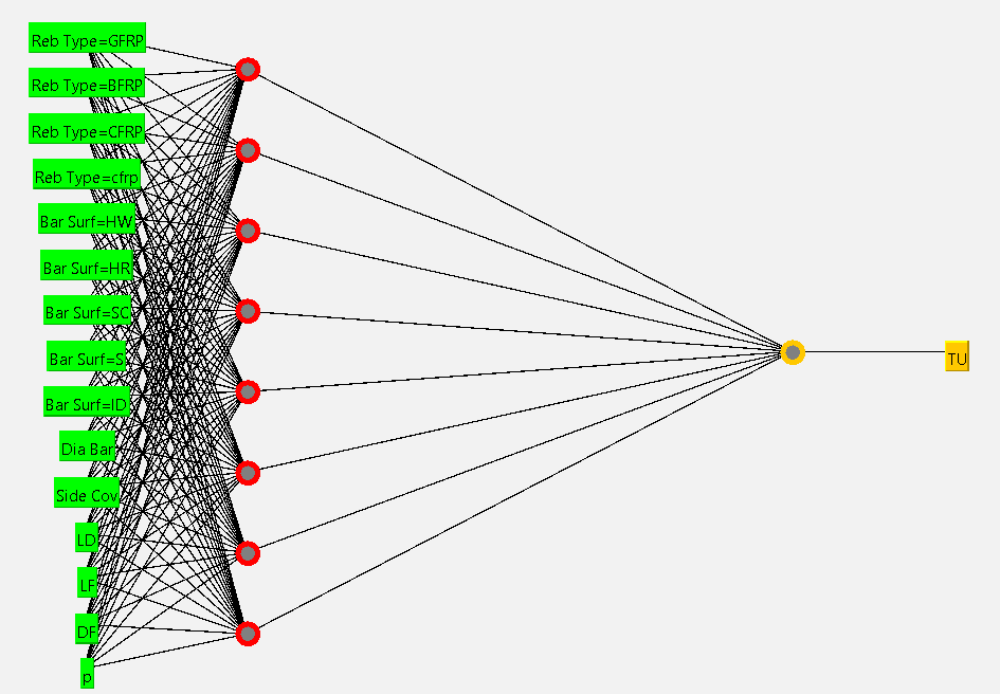


Figure 4. MLP diagram

2.3.3 Locally Weighted Learning (LWL)

It is an instance-based or lazy machine learning technique that performs prediction by giving higher importance to training samples located near the query instance. Unlike global learning algorithms that build a single generalized model from the entire dataset, LWL constructs a local model dynamically for each prediction using a subset of neighboring data points. The fundamental idea behind LWL is that complex nonlinear relationships within a dataset can be better captured by focusing on local patterns rather than assuming a single global function.

In LWL, a weight is allocated to each training sample according to its distance from the query point, typically using kernel functions such as Gaussian or inverse distance weighting. Instances closer to the query point receive higher weights and therefore have greater influence on the prediction. A simple regression or classification model is then fitted locally using these weighted instances to generate the final prediction. This approach enables LWL to adapt to variations in data distribution and effectively model nonlinear relationships. LWL offers advantages such as flexibility, simplicity, and the capacity

to process complex datasets without requiring extensive model training. However, it may require substantial computational resources when applied to large datasets because a local model must be constructed for each prediction. In civil engineering and materials research, LWL has been increasingly applied to predict material properties and structural performance due to its strong capability in modeling nonlinear and heterogeneous data patterns [34, 35].

3. Results and Discussion

The accuracy of the ML models was examed by using statistical performance indicators. The main evaluation metrics were the coefficient of determination (R^2), mean absolute error (MAE), root mean square error (RMSE), and mean absolute percentage error (MAPE). These metrics were selected because together, these metrics offer complementary perspectives on evaluation of the model. The (R^2) indicates how closely the predicted results agree with the experimental observations. A value close to 1 indicates high prediction accuracy. MAE represents the mean absolute deviation between the experimental and predicted bond strength values. RMSE gives higher weight to large errors and is useful for identifying models with large prediction deviations. MAPE represents the estimation deviation in percentage terms. The evaluation metrics were determined using the following equations:

$$R^2 = 1 - \frac{\sum_{i=1}^{n}(y_i - \hat{\bar{y}}_i)^2}{\sum_{i=1}^{n}(y_i - \bar{y}_i)^2}$$

$$MAE = \frac{1}{n}\sum_{i=1}^{n}|y_i - \hat{\bar{y}}_i|$$

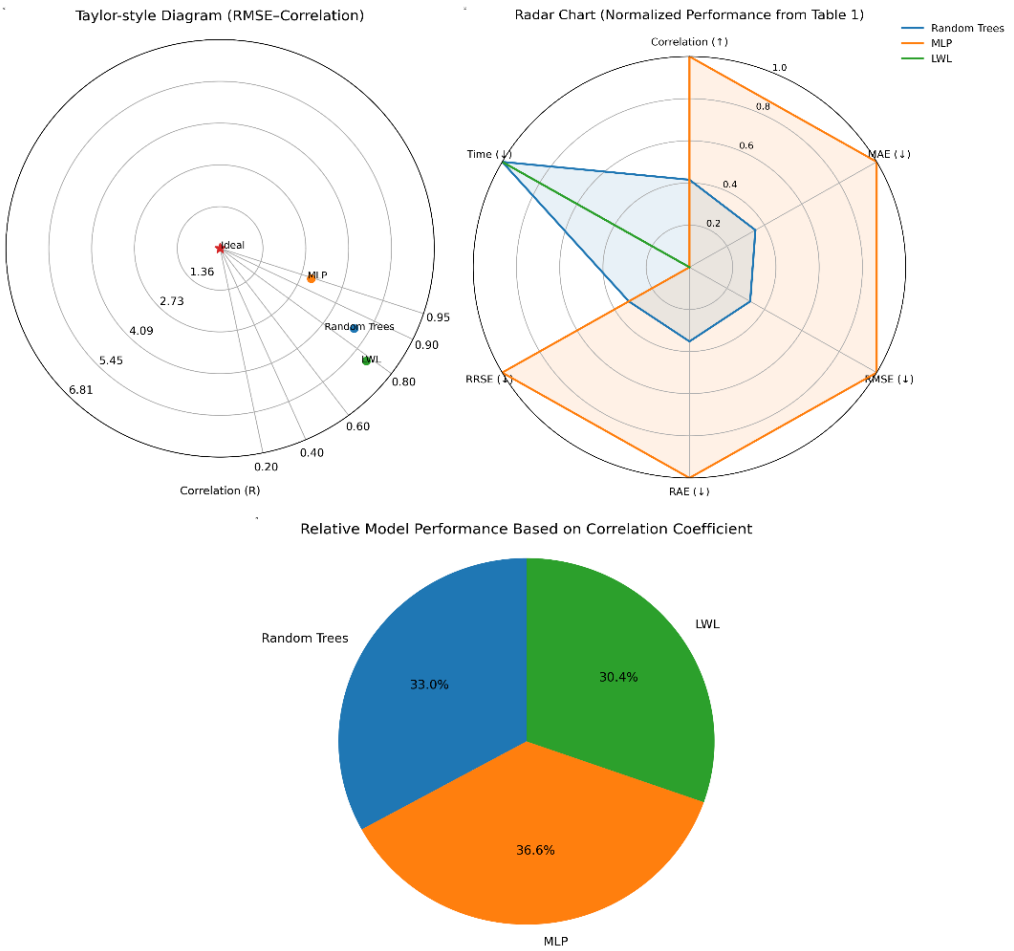
$$RMAE = \sqrt{\frac{1}{n}\sum_{i=1}^{n}(y_i - \hat{\bar{y}}_i)^2}$$

Table 2: Performace analysis table for the 3 MLs

ML	Correlation coefficient	Mean absolute error	Root mean squared error	Relative absolute error	Root relative squared error	Time Required (s)
Linear Regression	0.84	3.53	5.16	50.58%	54.42 %	0.063
Random Trees	0.85	3.64	4.99	51.81 %	52.35 %	0.16
MLP	0.94	2.30	3.06	32.84 %	32.09 %	0.13
LWL	0.78	4.36	5.92	62.13 %	62.05 %	0.6

Figure 5 shows a visual comparison of the models performance of the developed ML models for estimating the τ_u. This figure supports the numerical results reported in Table 2 and helps identify the best-performing model in a clearer way. The figure includes three complementary charts: a Taylor diagram, a radar chart, and a pie chart. These charts present different views of model performance, including prediction accuracy, error level, overall balance between evaluation metrics, and relative model performance. The compared models include (MLP), (RT), (LWL). Overall, Figure 5 indicates that MLP model achieved the highest predictive performance among the models examined.

Figure 5(a) shows the Taylor diagram, which provides an integrated statistical comparison between predicted and experimental bond strength values. This diagram simultaneously evaluates correlation coefficient and (RMSE), enabling a clear assessment of model accuracy. The Multi-Layer Perceptron (MLP) model lies nearest to the reference point, reflecting the strongest correlation and lowest prediction error among all models. The Random Trees model demonstrates moderate predictive capability, while the LWL model shows larger deviation from the reference point, reflecting lower prediction accuracy. Figure 5(b) presents a radar chart illustrating normalized performance indices of the several models across multiplstatistical metrics, including (R^2), (MAE), (RMSE), and (MAPE). The MLP model exhibits the most balanced and superior performance across all evaluation criteria, forming the largest enclosed area on the radar chart. Random Trees display moderate performance, whereas LWL occupies the smallest region, confirming its relatively weaker predictive capacity. Figure 5(c) displays a pie chart representing the relative contribution of each model based on correlation coefficient values. The chart highlights the dominant performance of the MLP model, followed by Random Trees and LWL. Collectively, the three subfigures provide a clear and integrated evaluation of model effectiveness, demonstrating that the MLP approach offers the most reliable and accurate predictive capability for modeling FRP–UHPC bond behavior.



Figuer 5: Performance comparison of ML models for estimating FRP–UHPC τ_u : (a) Taylor diagram, (b) radar chart, and (c) pie chart representation.

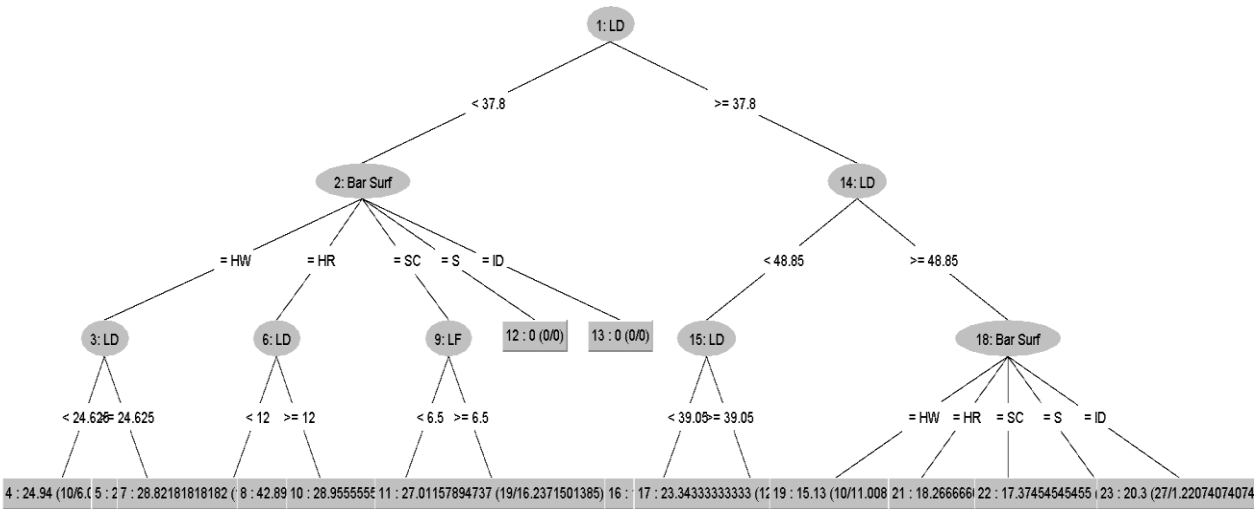


Figure 6: Random Trees diagram

Figure 6 presents the Random Trees model generated using the WEKA platform to estimate the τ_u of FRP bars embedded in UHPC. RT model was developed using the collected database of 183 specimens and the selected input variables, which are, test type, rebar type, bar surface condition, bar diameter d_b side cover c, embedment length L_d, fiber content ρ_f, UHPC compressive strength f_c', and FRP tensile strength f_r. The Random Trees model was constructed with a maximum depth of 3 and examed using 10-fold cross-validation. Trees structure shows that embedment length is the first splitting variable, with the main threshold occurring at approximately l_d = 37.8 mm. This indicates that embedment length plays a major important in controlling the predicted of τ_u. For shorter embedment lengths, bar surface condition becomes an important secondary parameter, where sand-coated bars and helically ribbed generally show higher predicted bond strength due to improved mechanical interlock and friction at the FRP–UHPC interface. For longer embedment lengths, the predicted bond strength generally decreases, which can be attributed to the nonuniform distribution of stress along the bonded depth and the resulting decrease in average bond stress. RT model further shows that surface type remains influential even in the longer embedment-length region, confirming that τ_u is controlled by the interaction between embedment length and bar surface condition. The model achieved a correlation coefficient of R^2 = 0.85, MAE of 3.64 MPa, and RMSE of 4.99 MPa, indicating reasonable prediction accuracy. Therefore, the Random Trees model provides both predictive capability and useful physical interpretation of the main parameters controlling FRP–UHPC bond behavior.

In addition , Figure 7 a,b,c,d compares the prediction performance of the developed ML models, including Linear Regression, Random Trees, Multi-Layer Perceptron, and Locally Weighted Learning, respectively. The comparison was based on the main statistical indicators, including (R^2), (MAE), (RMSE), and (MAPE). The results show that the nonlinear and local learning models generally performed better than the simple Linear Regression model. In particular, the MLP achieved the strongest overall results, yielding the highest correlation coefficient and the smallest error measures, indicating better agreement between the predicted and experimental bond strength values. Random Trees also showed good prediction accuracy and was able to capture part of the nonlinear behavior in the database. In contrast, Linear Regression and LWL showed relatively higher errors, suggesting that they were less effective for this dataset. Overall, the comparison confirms that the τ_u of FRP bars embedded in UHPC is controlled by nonlinear relationships between geometric and material parameters, and that local or tree-based ML models can provide more reliable predictions than simple linear modeling. In addition, SHAP analysis was employed to explain the ML model and determine the principal variables influencing the estimated τ_u, see Figure 8. It shows the influence of each input parameter on the predicted τ_u. The SHAP results showed that embedment length was the most

important parameter. This means that the bonded length has a the highest effective on the stress transfer between FRP bar and UHPC. When embedment length increases, the average bond stress may decrease because the bond stress is not distributed equally along the bonded depth. Bar surface condition was also important because ribbed, helically wound, or sand-coated bars can increase friction and mechanical interlock with UHPC. FRP tensile strength also affected τ_u because it is related to the mechanical capacity, and the resistance of the interface. Concrete cover thickness had an important effect because higher cover can give better confinement around the bar and delay splitting failure. Therefore, the SHAP results confirm that the τ_u of FRP bars in UHPC is mainly controlled by embedment length, surface condition, bar properties, and concrete confinement.

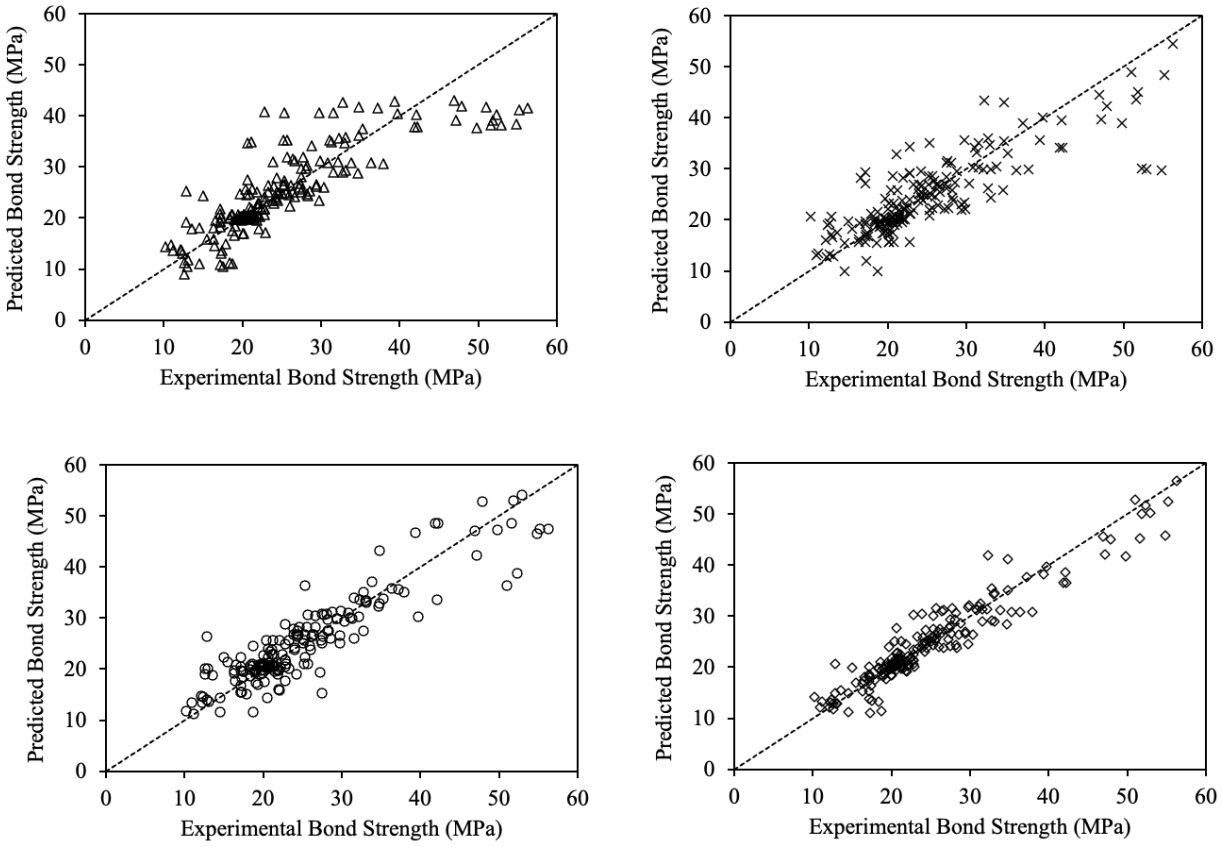


Figure 7. Assessment for ML models (a,b,c,and d) representing Linear Regression, Random Trees, Multi-Layer Perceptron, and Locally Weighted Learning, respectively.

The findings of this study agree with those reported in previous related research. The MLP model gave the highest prediction performance, which confirms that the τ_u of FRP bars embedded in UHPC is controlled by nonlinear relationships between the input parameters. This agrees with previous machine-learning studies, which showed that nonlinear models can predict FRP–concrete bond

behavior better than simple linear models. Also, the SHAP results showed that embedment length was the most important parameter, followed by bar surface condition, FRP tensile strength, and concrete cover. This agrees with experimental studies that reported the important effect of bonded length, surface roughness, mechanical interlock, and concrete confinement on bond strength. Therefore, the key contribution of this study is that it does not only predict the τ_u, but also explains the most important inputs affecting the FRP–UHPC bond behavior.

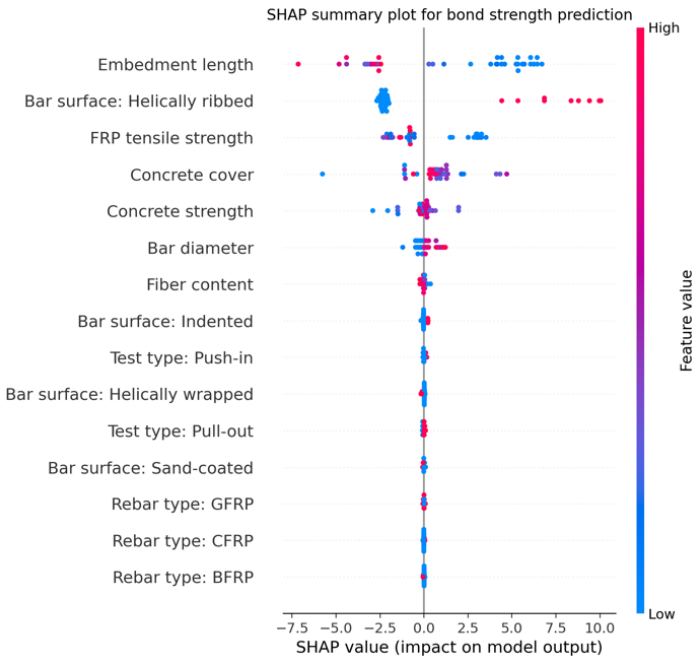


Figure 8: SHAP summary plot of bond strength

4. Conclusions

This study focused on the prediction and interpretation of the τ_u of FRP bars with UHPC. Research method was based on a data-driven machine-learning approach using a collected experimental database from previous studies. The database included 183 experimental tested samples with different FRP types, bar surface conditions, bar size, embedment lengths, concrete covers, fiber contents, UHPC compressive strengths, and FRP tensile strengths. The collected data were used to develop and compare Linear Regression, Random Trees, Multi-Layer Perceptron, and Locally Weighted Learning models. SHAP was also used to explain the influence of the variables on the predicted bond strength.

The comparison between the developed ML models showed that the Multi-Layer Perceptron provided the best prediction performance. The MLP model achieved a correlation coefficient of 0.9466, MAE of 2.30 MPa, RMSE of 3.06 MPa, RAE of 32.84%, and RRSE of 32.09%. Linear Regression and Random Trees showed moderate prediction accuracy, while LWL gave the lowest performance among

the evaluated models. The superior performance of MLP confirms that nonlinear learning models are more suitable for predicting FRP–UHPC bond strength because they can capture complex interactions between the selected input variables.

The results confirm that the bond behavior of FRP–UHPC systems is controlled by several interacting geometric, material, and surface-related parameters. This interaction shows that the bond response is nonlinear and cannot be fully represented by a simple linear relationship. The SHAP analysis showed that embedment length was the highest influence variable affecting the predicted τ_u, followed by bar surface condition, FRP tensile strength, and concrete cover. This indicates that the bonded length, surface configuration, bar properties, and confinement around the embedded bar contribute to the overall bond response.

Overall, the developed ML framework provides a useful data-driven approach for estimating the τ_u of FRP bars embedded in UHPC. The results also help identify the most important parameters controlling the bond response, which can support the development of UHPC-specific bond prediction models. However, the models should be used within the range of the collected database because the data were obtained from different experimental studies with different test methods, material properties, and specimen configurations.

Future work should focus on expanding the database by including more experimental results with different FRP types, bar surface configurations, UHPC mixture designs, fiber contents, cover thicknesses, and failure modes. Additional variables such as rib geometry, surface roughness, curing condition, and complete bond–slip response should also be included when available. This will improve model generalization, strengthen the physical interpretation of the ML results, and support the development of more reliable design-oriented bond models for FRP–UHPC structural systems.

Funding

The author declare that this research received no external funding.

Data Availability Statement

The data is available upon request to the corresponding author.

Conflicts of Interest

The authors declare no conflict of interest / or state any conflict if any.

References:

[1] H. Fergani, M. Di Benedetti, C. Miàs Oller, C. Lynsdale, and M. Guadagnini, "Durability and degradation mechanisms of GFRP reinforcement subjected to severe environments and sustained stress," *Constr. Build. Mater.*, vol. 170, pp. 637–648, May 2018, doi: 10.1016/j.conbuildmat.2018.03.092.

[2] L. Le Gué, P. Davies, M. Arhant, B. Vincent, and W. Verbouwe, "Basalt fibre degradation in seawater and consequences for long term composite reinforcement," *Compos. Part A Appl. Sci. Manuf.*, vol. 179, p. 108027, Apr. 2024, doi: 10.1016/j.compositesa.2024.108027.

[3] S. Abdal *et al.*, "Application of Ultra-High-Performance Concrete in Bridge Engineering: Current Status, Limitations, Challenges, and Future Prospects," *Buildings*, vol. 13, no. 1, p. 185, Jan. 2023, doi: 10.3390/buildings13010185.

[4] A. Qasem, Y. S. Sallam, H. Hossam Eldien, and B. H. Ahangarn, "Bond-slip behavior between ultra-high-performance concrete and carbon fiber reinforced polymer bars using a pull-out test and numerical modelling," *Constr. Build. Mater.*, vol. 260, p. 119857, Nov. 2020, doi: 10.1016/j.conbuildmat.2020.119857.

[5] C. S. Sun, N. Farzana, D. Kuruppuarachchi, M. Azimi, and H. Zhong, "Experimental and Analytical Studies of an Ultra-high Performance Concrete Beam Using Carbon Fiber Reinforced Polymer Bars," *Recent Prog. Mater.*, vol. 05, no. 02, pp. 1–17, May 2023, doi: 10.21926/rpm.2302019.

[6] X. Cao, D. He, K. Qian, F. Fu, X. Deng, and L. Wang, "Shear behavior of glass FRP bars-reinforced ultra-high performance concrete I-shaped beams," *Structural Concrete*, vol. 24, no. 1, pp. 1503–1520, Feb. 2023, doi: 10.1002/suco.202100801.

[7] Y. Luo, P. Liao, R. Pan, J. Zou, and X. Zhou, "Effect of bar diameter on bond performance of helically ribbed GFRP bar to UHPC," *Journal of Building Engineering*, vol. 91, p. 109577, Aug. 2024, doi: 10.1016/j.jobe.2024.109577.

[8] R. Kumar Tipu, V. Batra, Suman, K. S. Pandya, and V. R. Panchal, "Shear capacity prediction for FRCM-strengthened RC beams using Hybrid ReLU-Activated BPNN model," *Structures*, vol. 58, p. 105432, Dec. 2023, doi: 10.1016/j.istruc.2023.105432.

[9] M. Alhusban, M. Alhusban, and A. A. Alkhawaldeh, "The Efficiency of Using Machine Learning Techniques in Fiber-Reinforced-Polymer Applications in Structural Engineering," *Sustainability*, vol. 16, no. 1, p. 11, Dec. 2023, doi: 10.3390/su16010011.

[10] M. Kovačević, M. Hadzima-Nyarko, P. Petronijević, T. Vasiljević, and M. Radomirović, "Comparative Analysis of Machine Learning Models for Predicting Interfacial Bond Strength of Fiber-Reinforced Polymer-Concrete," *Computation*, vol. 13, no. 1, p. 17, Jan. 2025, doi: 10.3390/computation13010017.

[11] C. Arndt, C. Crusenberry, B. Heng, R. Butler, and S. TerMaath, "Reduced-Dimension Surrogate Modeling to Characterize the Damage Tolerance of Composite/Metal Structures," *Modelling*, vol. 4, no. 4, pp. 485–514, Nov. 2023, doi: 10.3390/modelling4040028.

[12] D.-Y. Yoo and Y.-S. Yoon, "Bond behavior of GFRP and steel bars in ultra-high-performance fiber-reinforced concrete," *Advanced Composite Materials*, vol. 26, no. 6, pp. 493–510, Nov. 2017, doi: 10.1080/09243046.2016.1197493.

[13] Y. Luo, P. Liao, R. Pan, J. Zou, and X. Zhou, "Effect of bar diameter on bond performance of helically ribbed GFRP bar to UHPC," *Journal of Building Engineering*, vol. 91, p. 109577, Aug. 2024, doi: 10.1016/j.jobe.2024.109577.

[14] C. Wang, Y. Jiao, J. Xing, and Y. Chen, "Bond Behavior of High-Strength Steel Rebar in Ultra-High-Performance Manufactured Sand Concrete: Experiment and Modelling," *Buildings*, vol. 14, no. 8, p. 2292, Jul. 2024, doi: 10.3390/buildings14082292.

[15] Y.-W. Chan and S.-H. Chu, "Effect of silica fume on steel fiber bond characteristics in reactive powder concrete," *Cem. Concr. Res.*, vol. 34, no. 7, pp. 1167–1172, Jul. 2004, doi: 10.1016/j.cemconres.2003.12.023.

[16] Z. Wu, C. Shi, and K. H. Khayat, "Influence of silica fume content on microstructure development and bond to steel fiber in ultra-high strength cement-based materials (UHSC)," *Cem. Concr. Compos.*, vol. 71, pp. 97–109, Aug. 2016, doi: 10.1016/j.cemconcomp.2016.05.005.

[17] L. Ke, K. Ma, Z. Chen, Y. Li, G. Chen, and Z. Feng, "Bond-slip and bond strength models for FRP bars embedded in ultra-high-performance concrete: A critical review," *Structures*, vol. 64, p. 106551, Jun. 2024, doi: 10.1016/j.istruc.2024.106551.

[18] Y. J. , & A. A. Kim, "Interface Shear between Ordinary Concrete and Ultra-High-Performance Concrete with Glass Fiber-Reinforced Polymer Reinforcing Bars," *ACI Struct. J.*, vol. 123, no. 3, May 2026, doi: 10.14359/51749317.

[19] Z. Shan, K. Liang, and L. Chen, "Bond behavior of helically wound FRP bars with different surface characteristics in fiber-reinforced concrete," *Journal of Building Engineering*, vol. 65, p. 105504, Apr. 2023, doi: 10.1016/j.jobe.2022.105504.

[20] K. Liang, L. Chen, Z. Shan, and R. K. L. Su, "Experimental and theoretical study on bond behavior of helically wound FRP bars with different rib geometry embedded in ultra-high-

performance concrete," *Eng. Struct.*, vol. 281, p. 115769, Apr. 2023, doi: 10.1016/j.engstruct.2023.115769.

[21] R. Pan, P. Liao, J. Zou, X. Zhou, and C. Li, "Experimental investigation on bond performance of helically ribbed GFRP rebar embedded in Ultra-high performance concrete," *Constr. Build. Mater.*, vol. 357, Nov. 2022, doi: 10.1016/j.conbuildmat.2022.129295.

[22] R. Pan, J. Zou, P. Liao, S. Dong, and J. Deng, "Effects of fiber content and concrete cover on the local bond behavior of helically ribbed GFRP bar and UHPC," *Journal of Building Engineering*, vol. 80, p. 107939, Dec. 2023, doi: 10.1016/j.jobe.2023.107939.

[23] F. Peng, H. Guan, J. Deng, and W. Xue, "Bond-slip behavior and model of sand-coated deformed GFRP bars in ultra-high-performance concrete," *Advances in Structural Engineering*, vol. 28, no. 8, pp. 1385–1402, Jun. 2025, doi: 10.1177/13694332241310113.

[24] F. AL-mahmoud, A. Castel, R. François, and C. Tourneur, "Effect of surface pre-conditioning on bond of carbon fibre reinforced polymer rods to concrete," *Cem. Concr. Compos.*, vol. 29, no. 9, pp. 677–689, Oct. 2007, doi: 10.1016/j.cemconcomp.2007.04.010.

[25] Y. J. Kim and J. Wang, "Interface of Ultra-High-Performance Concrete with Steel, Glass Fiber-Reinforced Polymer, and Basalt Fiber-Reinforced Polymer Reinforcing Bars," *ACI Struct. J.*, vol. 119, no. 3, pp. 3–15, May 2022, doi: 10.14359/51732640.

[26] F. Sayed Ahmad, G. Foret, and R. Le Roy, "Bond between carbon fibre-reinforced polymer (CFRP) bars and ultra high performance fibre reinforced concrete (UHPFRC): Experimental study," *Constr. Build. Mater.*, vol. 25, no. 2, pp. 479–485, Feb. 2011, doi: 10.1016/j.conbuildmat.2010.02.006.

[27] K. M. A. Hossain, D. Ametrano, and M. Lachemi, "Bond strength of GFRP bars in ultra-high strength concrete using RILEM beam tests," *Journal of Building Engineering*, vol. 10, pp. 69–79, Mar. 2017, doi: 10.1016/j.jobe.2017.02.005.

[28] N. Khalil and J. J. Assaad, "Bond properties between smooth carbon fibre-reinforced polymer bars and ultra-high performance concrete modified with polymeric latexes and fibres," *European Journal of Environmental and Civil Engineering*, vol. 26, no. 13, pp. 6211–6228, Oct. 2022, doi: 10.1080/19648189.2021.1934554.

[29] D. Y. Yoo, K. Y. Kwon, J. J. Park, and Y. S. Yoon, "Local bond-slip response of GFRP rebar in ultra-high-performance fiber-reinforced concrete," *Compos. Struct.*, vol. 120, pp. 53–64, Feb. 2015, doi: 10.1016/j.compstruct.2014.09.055.

[30] D.-Y. Yoo, J.-J. Park, S.-W. Kim, and Y.-S. Yoon, "Influence of reinforcing bar type on autogenous shrinkage stress and bond behavior of ultra high performance fiber reinforced concrete," *Cem. Concr. Compos.*, vol. 48, pp. 150–161, Apr. 2014, doi: 10.1016/j.cemconcomp.2013.11.014.

[31] J. Chen, Z. Fang, X. Chen, and R. Jiang, "Experimental study on lap behavior of CFRP indented bars in UHPC," *Constr. Build. Mater.*, vol. 344, p. 127959, Aug. 2022, doi: 10.1016/j.conbuildmat.2022.127959.

[32] A. Alatify and Y. J. Kim, "SP-363-8: Artificial Neural Networks for Prediction of Bond Strength between UHPC and FRP Reinforcing Bars."

[33] S. Abdal *et al.*, "Application of Ultra-High-Performance Concrete in Bridge Engineering: Current Status, Limitations, Challenges, and Future Prospects," *Buildings*, vol. 13, no. 1, p. 185, Jan. 2023, doi: 10.3390/buildings13010185.

[34] C. G. Atkeson, A. W. Moore, and S. Schaal, "Locally Weighted Learning," *Artif. Intell. Rev.*, vol. 11, no. 1–5, pp. 11–73, Feb. 1997, doi: 10.1023/A:1006559212014.

[35] "The WEKA workbench," in *Data Mining*, Elsevier, 2017, pp. 553–571. doi: 10.1016/B978-0-12-804291-5.00024-6.